Journal of Alzheimer's Disease xx (20xx) x–xx
DOI 10.3233/JAD-160833
IOS Press

Discriminative Properties of Hippocampal Hypoperfusion in Marijuana Users Compared to Healthy Controls: Implications for Marijuana Administration in Alzheimer's Dementia

Daniel G. Amen[a], Borhan Darmal[a], Cyrus A. Raji[b,*], Weining Bao[c], Lantie Jorandby[a], Somayeh Meysami[a] and Cauligi S. Raghavendra[c]
[a]*Amen Clinics Inc. Costa Mesa, CA, USA*
[b]*University of California San Francisco, San Francisco, CA, USA*
[c]*Department of Electrical Engineering, University of Southern California, Los Angeles, CA, USA*

Accepted 19 October 2016

Abstract.
Background: Few studies have evaluated the impact of marijuana use on regional cerebral blood flow.
Objective: To determine whether perfusion in specific brain regions on functional neuroimaging, including those affected by Alzheimer's disease pathology, are abnormal in marijuana users compared to controls.
Method: Persons with a diagnosis of cannabis use disorder by DSM-IV and DSM-V criteria ($n = 982$) were compared to controls ($n = 92$) with perfusion neuroimaging with SPECT at rest and at a concentration task. Perfusion estimates were quantified using a standard atlas. Cerebral perfusion differences were calculated using one-way ANOVA. Diagnostic separation was determined with discriminant analysis of all subjects. Feature selection with a minimum redundancy maximum relevancy (mRMR) identified predictive regions in a subset of marijuana users ($n = 436$) with reduced psychiatric co-morbidities.
Results: Marijuana users showed lower cerebral perfusion on average ($p < 0.05$). Discriminant analysis distinguished marijuana users from controls with correct classification of 96% and leave one out cross-validation of 92%. With concentration SPECT regions, there was correct classification of 95% with a leave-one-out cross validation of 90%. AUC analysis for concentration SPECT regions showed 95% accuracy, 90% sensitivity, and 83% specificity. The mRMR analysis showed right hippocampal hypoperfusion on concentration SPECT imaging was the most predictive in separating marijuana subjects from controls.
Conclusion: Multiple brain regions show low perfusion on SPECT in marijuana users. The most predictive region distinguishing marijuana users from healthy controls, the hippocampus, is a key target of Alzheimer's disease pathology. This study raises the possibility of deleterious brain effects of marijuana use.

Keywords: Hippocampus, imaging, marijuana, SPECT

INTRODUCTION

Reported rates of marijuana use have more than doubled in the past decade [1]. Medical marijuana is now legal in nearly half of US states [2], increasing

*Correspondence to: Cyrus A. Raji, MD, PhD, University of California San Francisco, San Francisco, CA, USA. E-mail: cyrusraji@gmail.com.

access to the drug for current and potential future users. As marijuana is often portrayed as a harmless drug in popular culture, a conception that marijuana is a benign substance with therapeutic value for some diseases is commonplace [3]. Concurrently, 10 of the 24 US states that have legalized marijuana include Alzheimer's dementia (AD) as a valid indication for its medical use [4]. This therapeutic application of marijuana exists despite lack of conclusive evidence regarding benefit of this drug in a variety of disorders including AD [5, 6]. Understanding the relevance of marijuana use for AD necessitates investigation of its effects on the human brain compared to non-marijuana users. Currently, few studies have been published analyzing the impact that marijuana use has on the human brain.

The available literature assessing the impact of marijuana use on the brain has predominantly shown depressive effects on neurophysiology [7, 8]. A recent study using positron emission tomography (PET) imaging demonstrated decreased dopamine release in the striatum, a region of the brain that is involved in working memory, impulsive behavior, and attention [9]. These results show that heavy marijuana use has an effect on dopamine release similar to hard drugs, such as heroin and cocaine. Another study using diffusion tensor imaging showed damage to the corpus callosum, a white matter tract responsible for connecting the left and right hemispheres, in 59 individuals who smoke high-potency cannabis [10]. A third study using structural magnetic resonance imaging (MRI) demonstrated a decrease in orbitofrontal cortex volume in chronic marijuana users [11].

While a recent study suggested that marijuana can reduce amyloid-β-related inflammation by activation of cannabinoid receptors [12], other imaging studies have suggested structural damage in areas vulnerable to AD pathology. Several studies in chronic cannabis users showed decreased hippocampal volumes related to the amount of cannabis used [13–15]. Most striking is that these structural changes are shown to be long lasting as the volume reductions seen with heavy use persisted after six months of abstinence.

There is lack of functional brain imaging data in large cohorts of persons with history of marijuana use. Such information is important given the improved sensitivity of functional imaging to physiological alterations. The purpose of this study is to further investigate specific regions of the brain that are neurophysiologically impaired in marijuana users compared to non-users. We hypothesize that marijuana users will exhibit hypoperfusion compared to controls on brain SPECT, including areas known to be affected by AD pathology such as the hippocampus.

METHODS

Study participants

This study was conducted in accordance with the STARD guidelines (http://www.stard-statement.org/). All subjects were obtained for retrospective analysis from a large multisite psychiatric database, involving 26,268 patients who came for evaluation of complex, treatment resistant issues to one of nine outpatient clinics (Newport Beach, Costa Mesa, Fairfield, and Brisbane, CA; Tacoma and Bellevue, WA; Reston, VA; Atlanta, GA; and New York, NY) between 1995–2014. Diagnoses were made by board certified or eligible psychiatrists, using all of the data available to them, including detailed clinical history, mental status examination, and DSM-IV or V criteria, consistent with the current standard of care. Anonymized data was extracted from a research database using a data mining technique within a protocol deemed appropriate by an independent IRB IntegReview (http://www.integreview.com/) to be exempt from human subjects review in accordance with 45 CFR 46.101(b)(4) (IRB #004).

Included in the database were healthy adult volunteers who had single-photon emission computed tomography (SPECT) studies. The exclusion criteria for the healthy subjects were: 1) current or past evidence of psychiatric illnesses as determined by clinical history, mental status examinations, and the Structured Clinical Interview for Diagnosis for DSM-IV; 2) current reported medical illnesses or medication; 3) history of brain trauma; 4) current or past drug or alcohol abuse; 5) first degree relative with a psychiatric illness. Written informed consent was obtained from all healthy subjects under an approved IRB protocol (WIRB # 20021714). A subset of 982 (ages 18–84, males 83%) patients with a diagnosis of cannabis use disorder by DSM-IV and DSM-V criteria were identified and compared to a healthy control population ($n = 92$, age 18–84, 42% male) with perfusion neuroimaging with SPECT. The most common comorbidities in in the cannabis use group were i) attention-deficit/hyperactivity disorder (62%); ii) traumatic brain injury (TBI) (47%); iii) and major depressive disorder (35%).

SPECT neuroimaging acquisition

All subjects received functional perfusion neuroimaging with SPECT as described in previous studies [16, 17]. Briefly, brain SPECT scans were performed using a high resolution Picker (Philips) Prism XP 3000 triple-headed gamma camera (Picker Int. Inc., Ohio Nuclear Medicine Division, Bedford Hills, OH, USA) with low energy high-resolution fan beam collimators. Each participant received an age and weight appropriate dose of technetium–99 m hexamethylpropyleneamine (HMPAO). For rest scans, the injection was done intravenously in a quiet room with low level ambient lighting while awake with eyes open. Brain SPECT scanning was then done 30 minutes after injection. For concentration scans, patients were injected three minutes after starting the Conners Continuous Performance Test (Conners Continuous Performance Test, CCPT-II, Multi-Health Systems, Toronto, Ontario). SPECT scanning was subsequently done 30 minutes after injection.

Data was acquired in 128×128 matrices, resulting in 120 images per scan with each image separated by three degrees spanning 360 degrees. The original image matrix obtained at $128 \times 128 \times 29$ with voxel sizes of 2.16 mm × 2.16 mm × 6.48 mm were transformed and resliced to a $79 \times 95 \times 68$ matrix with voxel sizes of 2 mm × 2 mm × 2 mm consistent with the Montreal Neurological Institute template [18]. Images were smoothed using an 8 mm FWHM isotropic Gaussian kernel with slice thickness of 6 mm. A low pass filter was applied with a high cutoff. Chang attenuation correction was performed [19]. The total number of counts in a given brain SPECT study was 10 million. Transaxial slices oriented horizontal to the AC-PC line were created along with coronal and sagittal images at 6.6 mm apart, unsmoothed.

Perfusion quantification

Regional cerebral blood flow was quantified in all 256 regions (128 baseline, 128 concentration) using a standard neuroanatomical atlas, the AAL atlas [20], as previously described [16, 17]. To summarize, counts in each region of interest were quantified using trimmed means. Trimmed means were calculated using all scores in a 98% confidence interval ($-2.58 < Z < -2.58$). Perfusion for each region was then estimated with the trimmed mean using the following formula:

T = 10*((subject ROI_mean –trimmed regional_avg)/trimmed regional_stdev)+50.

Predictive data analytics

All statistical analyses were performed in Statistical Package for Social Science (SPSS, version 22, IBM, Armonk, NY) and were controlled for age, gender, and race. To identify specific brain regions that may be predictive in distinguishing marijuana users from controls, a one-way ANOVA was conducted to such areas from the AAL atlas [20] of computed perfusion values [21]. Multiple pairwise comparisons were accounted for with a false discovery rate [22]. We hypothesized that regional cerebral hypoperfusion, including in areas known to be affected by AD such as the hippocampus, would reliably classify marijuana users. For the hippocampus specifically, Cohen's D effect size calculations were rendered based on mean differences and standard deviations [23].

Hypoperfused brain areas in the marijuana group were then used to classify this group from controls with discriminant analysis using a leave-one-out cross validation [24]. For this step, baseline perfusion measures were inputted into the discriminant analysis followed by a separate analysis with concentration SPECT regions. This was followed by extraction of predicted probabilities from this model. These probabilities were then used to determine diagnostic sensitivity, specificity, and accuracy with receiver operating characteristic (ROC) and area under the curve (AUC) analyses.

Feature selection using a reduced co-morbidity analysis

Because almost half of the original sample had persons with TBI, we reduced co-morbidity burden by excluding these subjects in this analysis as TBI could potentially mimic hypoperfusion seen in in our marijuana subjects. This resulted in 436 marijuana users compared to 92 controls. A different machine learning algorithm, support vector machine (SVM) was applied [25]. As part of this analysis an oversampling method was applied, k = 0.5. A minimum redundancy maximum relevancy (mRmR) method was then applied to identify the top 10 most predictive SPECT regions (baseline or concentration) [26]. All 256 ROIs, 128 baseline and 128 concentration, were inputted as variables into the SVM mRMR analysis.

RESULTS

All regions with lower perfusion on both baseline and concentration SPECT scans are listed in Table 1. Of the 256 regions assessed, the majority was statistically significant in showing lower perfusion among marijuana users compared to controls ($p < 0.05$). Hypoperfused regions in marijuana users compared to controls include areas known to be targeted by AD pathology including: i) hippocampus; ii) parahippocampal gyrus; iii) precuneus; iv) posterior cingulate; and v) medial temporal lobes.

The discriminant analysis of 982 marijuana users from 92 controls using baseline SPECT regions yielded a correct classification rate of 96% with the leave-one-out cross validation at 92%. The corresponding accuracy of the linear discriminant probabilities in identifying marijuana users from controls was 95% based upon AUC analysis with 90% sensitivity and 85% specificity. When using concentration SPECT regions in the discriminant analysis, the results were similar with a correct classification of 95% with a leave-one-out cross validation of 90%. The AUC analysis for concentration SPECT regions from the discriminant analysis was also similar to the baseline regions with 95% accuracy, 90% sensitivity, and 83% specificity.

The top 10 predictive regions from the 256 ROIs (128 baseline and 128 concentration) inputted into the subgroup SVM mRMR analysis are listed in Table 2. Notably, the right hippocampus on concentration SPECT scan is the most predictive region in distinguishing marijuana users from controls. Hippocampal perfusion in marijuana users is 13% lower on concentration scans compared to controls ($F = 81.8$ for left hippocampus, $p < 0.001$; $F = 99.4$ for right hippocampus, $p < 0.001$) with a large effect size (Cohen's $D = 0.99$ for left and 1.03 for right). Baseline hippocampal perfusion was reduced by about 17% in marijuana users compared to controls ($F = 114.3$, $p < 0.001$ for left hippocampus; $F = 123.9$, $p < 0.001$ for right hippocampus). The results also had large effect size (Cohen's $D = 1.1$ for left hippocampus and 1.2 for right hippocampus).

DISCUSSION

Regional, specifically hippocampal, hypoperfusion in marijuana users reliably distinguishes this group from healthy controls. The right hippocampus during concentration task was the single most predictive region in distinguishing marijuana users from their normal counterparts. This finding is important given a prior multi-modal study showing 3% reduced hippocampal volume in cannabis users compared to non-users and increased N-acetylaspartate on magnetic resonance spectroscopy [27]. Another study of 15 chronic cannabis users utilized functional MRI (fMRI) to reveal impaired activation during learning tasks compared to non-users [28]. Individuals who use both marijuana and nicotine also have lower hippocampal volumes and lower immediate/delayed story recall compared to non-users [29]. Additionally, cannabis use is thought to interfere with memory formation by inhibiting long-term potentiation [30].

While the hippocampus is the most predictive region in our study, it is also seen as abnormal in marijuana users based on the literature. Other brain areas are affected as well. A recent systematic review concluded that structural and functional defects in the cerebellum are a common feature in neuroimaging studies of cannabis users [31]. This is also seen with our work given that three of the ten most predictive regions in our results were cerebellar sub-regions. These findings are consistent with descriptions in the literature of coordination deficits in marijuana users [32].

Pallidum hypoperfusion found in our study is corroborated by subcortical white matter abnormalities seen on diffusion tensor imaging data of marijuana users in the Human Connectome Project [33]. An fMRI study also showed attenuation of frontal-subcortical circuits in heavy cannabis users as well as reduced performance on motivation driven tasks [34]. The anterior temporal lobe hypoperfusion detected in our study is also consistent with prior fMRI data showing temporal lobe deactivation as a function of negative emotionality in marijuana users [35].

Several studies of perfusion imaging in marijuana users have shown similar results compared to ours. A small O15 PET study in a sample of 12 marijuana users used a randomized clinical trial design to examine brain perfusion before and after marijuana. The study results found frontal, temporal, and occipital lobe hypoperfusion—all findings concordant with our study [36]. That same study showed increased perfusion in several regions, such as the cerebellum, that we did not observe in our larger sample. Another comparatively recent paper from the same group showed marijuana users recruited the cerebellum in a monetary decision task on O15 PET imaging. [37]. However, a recent study showed reduced FDG-PET glucose metabolism in marijuana users in the

Table 1
Perfusion differences between marijuana users and controls

Brain region	Mean Perfusion in Marijuana	Standard Deviation in Marijuana	Mean Perfusion in Control	Standard Deviation in Control	% Difference	F-value	*p*-value
T_Baseline_Amygdala_L Normalized (ROI) AAL Atlas	49.36669	6.112331	57.29246	8.238188	14.86	99.274	0.000
T_Baseline_Amygdala_R Normalized (ROI) AAL Atlas	48.85348	5.977822	57.42231	9.069583	16.13	110.564	0.000
T_Baseline_Angular_L Normalized (ROI) AAL Atlas	47.37826	4.951218	50.91824	6.989043	7.20	29.153	0.000
T_Baseline_Angular_R Normalized (ROI) AAL Atlas	43.58048	4.734176	44.91513	5.942004	3.02	4.931	0.027
T_Baseline_Calcarine_L Normalized (ROI) AAL Atlas	51.37545	5.031012	55.36625	7.265667	7.48	35.251	0.000
T_Baseline_Calcarine_R Normalized (ROI) AAL Atlas	52.24926	5.68438	59.30704	8.926656	12.65	80.537	0.000
T_Baseline_Caudate_L Normalized (ROI) AAL Atlas	48.6602	6.320132	56.1587	8.644014	14.31	82.221	0.000
T_Baseline_Caudate_R Normalized (ROI) AAL Atlas	50.18716	6.287653	58.3214	8.68691	14.99	97.022	0.000
T_Baseline_Cerebellum_10_L Normalized (ROI) AAL Atlas	38.04574	6.141007	42.20295	7.62846	10.36	28.626	0.000
T_Baseline_Cerebellum_10_R Normalized (ROI) AAL Atlas	35.52064	6.571395	38.54453	7.514499	8.17	13.922	0.000
T_Baseline_Cerebellum_3_L Normalized (ROI) AAL Atlas	50.82809	6.559175	57.59797	9.629127	12.49	58.901	0.000
T_Baseline_Cerebellum_3_R Normalized (ROI) AAL Atlas	49.70841	5.863644	55.79712	8.896435	11.54	58.019	0.000
T_Baseline_Cerebellum_4_5_L Normalized (ROI) AAL Atlas	53.44867	6.43342	61.13994	10.039613	13.42	75.079	0.000
T_Baseline_Cerebellum_4_5_R Normalized (ROI) AAL Atlas	54.35946	6.34349	61.56507	10.188184	12.43	66.079	0.000
T_Baseline_Cerebellum_6_L Normalized (ROI) AAL Atlas	59.83567	7.119795	68.57752	10.552287	13.62	82.71	0.000
T_Baseline_Cerebellum_6_R Normalized (ROI) AAL Atlas	58.48637	6.969697	66.94536	10.032157	13.49	82.738	0.000
T_Baseline_Cerebellum_7b_L Normalized (ROI) AAL Atlas	39.17156	5.90116	36.70368	5.617071	6.51	12.631	0.000
T_Baseline_Cerebellum_7b_R Normalized (ROI) AAL Atlas	32.02763	5.779296	29.56377	5.701352	8.00	12.913	0.000
T_Baseline_Cerebellum_8_L Normalized (ROI) AAL Atlas	43.72935	5.969232	42.28828	6.704199	3.35	3.872	0.050
T_Baseline_Cerebellum_8_R Normalized (ROI) AAL Atlas	40.12962	5.640795	38.43994	6.696728	4.30	5.768	0.017
T_Baseline_Cerebellum_9_L Normalized (ROI) AAL Atlas	48.57332	6.515605	49.83271	8.459127	2.56	2.265	0.133
T_Baseline_Cerebellum_9_R Normalized (ROI) AAL Atlas	48.64528	6.22475	50.04012	8.332316	2.83	2.979	0.085
T_Baseline_Cerebellum_Crus1_L Normalized (ROI) AAL Atlas	50.40691	5.784134	50.9665	6.726173	1.10	0.609	0.436
T_Baseline_Cerebellum_Crus1_R Normalized (ROI) AAL Atlas	44.64358	5.148788	44.38834	6.394592	0.57	0.154	0.695
T_Baseline_Cerebellum_Crus2_L Normalized (ROI) AAL Atlas	38.63843	6.43554	35.20117	6.033216	9.31	20.74	0.000
T_Baseline_Cerebellum_Crus2_R Normalized (ROI) AAL Atlas	33.67005	5.296017	30.96151	5.098662	8.38	18.794	0.000
T_Baseline_Cingulum_Ant_L Normalized (ROI) AAL Atlas	53.75003	7.296637	63.26544	10.094512	16.26	98.488	0.000
T_Baseline_Cingulum_Ant_R Normalized (ROI) AAL Atlas	49.99914	6.700864	58.60406	9.601516	15.85	92.957	0.000
T_Baseline_Cingulum_Mid_L Normalized (ROI) AAL Atlas	55.45845	6.693783	63.47313	9.412818	13.48	82.001	0.000
T_Baseline_Cingulum_Mid_R Normalized (ROI) AAL Atlas	53.34425	6.490052	61.04861	9.204779	13.47	80.075	0.000
T_Baseline_Cingulum_Post_L Normalized (ROI) AAL Atlas	53.22738	6.927181	62.73646	10.905316	16.40	98.231	0.000
T_Baseline_Cingulum_Post_R Normalized (ROI) AAL Atlas	48.47364	6.624928	57.56844	10.89309	17.15	94.48	0.000
T_Baseline_Cuneus_L Normalized (ROI) AAL Atlas	49.42842	5.587541	52.70578	6.743228	6.42	21.893	0.000
T_Baseline_Cuneus_R Normalized (ROI) AAL Atlas	49.52857	5.564847	53.71048	6.872707	8.10	35.41	0.000
T_Baseline_Frontal_Inf_Oper_L Normalized (ROI) AAL Atlas	51.67557	6.082221	57.75121	8.08497	11.10	59.506	0.000
T_Baseline_Frontal_Inf_Oper_R Normalized (ROI) AAL Atlas	50.22173	5.409387	54.63944	7.332006	8.43	39.217	0.000
T_Baseline_Frontal_Inf_Orb_L Normalized (ROI) AAL Atlas	48.65905	5.127709	50.54043	7.041872	3.79	7.839	0.005
T_Baseline_Frontal_Inf_Orb_R Normalized (ROI) AAL Atlas	45.7083	4.767966	46.36443	6.257069	1.43	1.14	0.286
T_Baseline_Frontal_Inf_Tri_L Normalized (ROI) AAL Atlas	50.65315	5.57055	55.43904	7.227324	9.02	44.776	0.000
T_Baseline_Frontal_Inf_Tri_R Normalized (ROI) AAL Atlas	46.87252	4.738548	49.38903	6.429275	5.23	16.571	0.000

(*Continued*)

Table 1
(*Continued*))

Brain region	Mean Perfusion in Marijuana	Standard Deviation in Marijuana	Mean Perfusion in Control	Standard Deviation in Control	% Difference	F-value	*p*-value
T_Baseline_Frontal_Mid_L Normalized (ROI) AAL Atlas	47.67076	5.069064	50.20287	6.247762	5.17	15.666	0.000
T_Baseline_Frontal_Mid_Orb_L Normalized (ROI) AAL Atlas	54.52962	6.17766	58.49839	7.617183	7.02	25.906	0.000
T_Baseline_Frontal_Mid_Orb_L_9 Normalized (ROI) AAL Atlas	46.73683	5.237633	46.44804	7.755249	0.62	0.167	0.683
T_Baseline_Frontal_Mid_Orb_R Normalized (ROI) AAL Atlas	52.1573	6.151681	58.01965	7.492432	10.64	57.455	0.000
T_Baseline_Frontal_Mid_Orb_R_10 Normalized (ROI) AAL Atlas	43.69696	5.656589	41.59493	7.651218	4.93	8.132	0.005
T_Baseline_Frontal_Mid_R Normalized (ROI) AAL Atlas	45.83314	4.777828	47.38821	6.043344	3.34	6.539	0.011
T_Baseline_Frontal_Sup_L Normalized (ROI) AAL Atlas	43.90665	4.683009	45.38983	5.34503	3.32	6.602	0.011
T_Baseline_Frontal_Sup_Medial_L Normalized (ROI) AAL Atlas	48.31012	5.3936	50.04348	6.025495	3.52	6.882	0.009
T_Baseline_Frontal_Sup_Medial_R Normalized (ROI) AAL Atlas	46.32877	5.148241	47.83988	5.644116	3.21	5.801	0.016
T_Baseline_Frontal_Sup_Orb_L Normalized (ROI) AAL Atlas	48.00895	5.111681	50.0328	7.299953	4.13	8.86	0.003
T_Baseline_Frontal_Sup_Orb_R Normalized (ROI) AAL Atlas	46.29076	4.934679	47.10389	7.60869	1.74	1.441	0.231
T_Baseline_Frontal_Sup_R Normalized (ROI) AAL Atlas	43.58097	4.658017	45.12307	5.543593	3.48	7.035	0.008
T_Baseline_Fusiform_L Normalized (ROI) AAL Atlas	50.97234	5.70577	56.10421	7.274363	9.59	49.665	0.000
T_Baseline_Fusiform_R Normalized (ROI) AAL Atlas	49.98494	5.813409	54.92465	7.5297	9.42	43.85	0.000
T_Baseline_Heschl_L Normalized (ROI) AAL Atlas	56.03541	6.848499	64.11262	9.534253	13.45	80.176	0.000
T_Baseline_Heschl_R Normalized (ROI) AAL Atlas	56.71999	7.424798	65.60007	10.340104	14.52	82.426	0.000
T_Baseline_Hippocampus_L Normalized (ROI) AAL Atlas	48.71561	5.86743	57.04141	8.325666	15.75	114.371	0.000
T_Baseline_Hippocampus_R Normalized (ROI) AAL Atlas	48.47854	6.034483	57.54018	8.920905	17.09	123.973	0.000
T_Baseline_Insula_L Normalized (ROI) AAL Atlas	55.06146	6.744448	62.89178	9.25741	13.28	78.523	0.000
T_Baseline_Insula_R Normalized (ROI) AAL Atlas	56.02237	6.874326	63.91265	9.387912	13.16	77.036	0.000
T_Baseline_Lingual_L Normalized (ROI) AAL Atlas	54.26051	5.806964	60.97005	8.540389	11.65	73.706	0.000
T_Baseline_Lingual_R Normalized (ROI) AAL Atlas	53.1902	5.863219	60.24968	8.778842	12.45	78.872	0.000
T_Baseline_Occipital_Inf_L Normalized (ROI) AAL Atlas	44.905	5.349338	45.02268	6.337261	0.26	0.031	0.860
T_Baseline_Occipital_Inf_R Normalized (ROI) AAL Atlas	38.40352	5.413964	36.57779	6.395581	4.87	7.333	0.007
T_Baseline_Occipital_Mid_L Normalized (ROI) AAL Atlas	45.54728	4.825798	47.9709	6.702075	5.18	14.565	0.000
T_Baseline_Occipital_Mid_R Normalized (ROI) AAL Atlas	42.16994	5.018126	42.25995	5.940799	0.21	0.021	0.886
T_Baseline_Occipital_Sup_L Normalized (ROI) AAL Atlas	43.5834	4.934667	45.32753	6.217575	3.92	7.73	0.006
T_Baseline_Occipital_Sup_R Normalized (ROI) AAL Atlas	43.79968	5.026455	45.33971	5.742336	3.46	6.175	0.013
T_Baseline_Olfactory_L Normalized (ROI) AAL Atlas	51.2907	6.099347	58.09372	8.611165	12.44	70.94	0.000
T_Baseline_Olfactory_R Normalized (ROI) AAL Atlas	52.25316	6.299174	58.93389	8.571795	12.02	65.947	0.000
T_Baseline_Pallidum_L Normalized (ROI) AAL Atlas	55.12202	7.400181	66.158	10.835831	18.20	123.224	0.000
T_Baseline_Pallidum_R Normalized (ROI) AAL Atlas	58.29287	8.219952	69.34062	11.659257	17.31	102.636	0.000
T_Baseline_Paracentral_Lobule_L Normalized (ROI) AAL Atlas	40.05218	4.933879	43.71877	6.394995	8.75	33.525	0.000
T_Baseline_Paracentral_Lobule_R Normalized (ROI) AAL Atlas	42.01043	4.838896	45.9294	6.819798	8.91	37.453	0.000
T_Baseline_ParaHippocampal_L Normalized (ROI) AAL Atlas	45.47443	5.103483	50.25239	6.739881	9.98	52.513	0.000
T_Baseline_ParaHippocampal_R Normalized (ROI) AAL Atlas	48.41976	5.584162	54.83919	7.59873	12.43	77.481	0.000
T_Baseline_Parietal_Inf_L Normalized (ROI) AAL Atlas	47.94481	5.250041	51.2983	7.205478	6.76	23.77	0.000
T_Baseline_Parietal_Inf_R Normalized (ROI) AAL Atlas	43.87391	5.378813	44.99445	6.641514	2.52	2.722	0.100
T_Baseline_Parietal_Sup_L Normalized (ROI) AAL Atlas	38.8723	4.586032	39.66757	5.592882	2.03	1.901	0.169
T_Baseline_Parietal_Sup_R Normalized (ROI) AAL Atlas	34.20693	4.205333	33.36296	4.796871	2.50	2.652	0.104
T_Baseline_Postcentral_L Normalized (ROI) AAL Atlas	45.03062	4.807055	48.88852	6.56026	8.22	37.682	0.000
T_Baseline_Postcentral_R Normalized (ROI) AAL Atlas	41.94542	4.325556	44.32524	6.068668	5.52	17.344	0.000

T_Baseline_Precentral_L Normalized (ROI) AAL Atlas	45.93774	4.794493	50.12627	6.781166	8.72	43.46	0.000
T_Baseline_Precentral_R Normalized (ROI) AAL Atlas	43.38155	4.349247	46.18569	6.136912	6.26	23.715	0.000
T_Baseline_Precuneus_L Normalized (ROI) AAL Atlas	47.59377	5.348351	52.76986	7.4616	10.31	53.898	0.000
T_Baseline_Precuneus_R Normalized (ROI) AAL Atlas	49.10763	5.613133	55.56633	7.990696	12.34	75.014	0.000
T_Baseline_Putamen_L Normalized (ROI) AAL Atlas	59.04499	7.497782	68.98028	10.533365	15.52	100.508	0.000
T_Baseline_Putamen_R Normalized (ROI) AAL Atlas	59.5658	7.539293	68.8708	10.540324	14.49	87.517	0.000
T_Baseline_Rectus_L Normalized (ROI) AAL Atlas	52.06473	5.979088	55.3137	8.35761	6.05	16.967	0.000
T_Baseline_Rectus_R Normalized (ROI) AAL Atlas	51.21163	5.744114	55.01977	8.507161	7.17	24.128	0.000
T_Baseline_Rolandic_Oper_L Normalized (ROI) AAL Atlas	53.75129	6.42739	61.52823	9.360674	13.49	81.47	0.000
T_Baseline_Rolandic_Oper_R Normalized (ROI) AAL Atlas	52.20951	5.912713	59.06247	8.844382	12.32	73.144	0.000
T_Baseline_Supp_Motor_Area_L Normalized (ROI) AAL Atlas	45.2619	5.075356	49.13337	7.1917	8.20	33.086	0.000
T_Baseline_Supp_Motor_Area_R Normalized (ROI) AAL Atlas	45.25485	5.047343	49.49263	7.195655	8.95	39.896	0.000
T_Baseline_SupraMarginal_L Normalized (ROI) AAL Atlas	50.57601	5.765638	55.99627	8.176482	10.17	50.223	0.000
T_Baseline_SupraMarginal_R Normalized (ROI) AAL Atlas	47.49624	5.291321	50.50489	7.588427	6.14	18.212	0.000
T_Baseline_Temporal_Inf_Ant_L Normalized (ROI) AAL Atlas	40.57946	6.318665	38.0372	7.949163	6.47	10.028	0.002
T_Baseline_Temporal_Inf_Ant_R Normalized (ROI) AAL Atlas	36.43539	6.252945	33.69082	6.592023	7.83	13.247	0.000
T_Baseline_Temporal_Inf_Mid_L Normalized (ROI) AAL Atlas	44.33335	5.453387	45.23614	6.617098	2.02	1.738	0.188
T_Baseline_Temporal_Inf_Mid_R Normalized (ROI) AAL Atlas	40.68491	5.077737	40.74424	6.112053	0.15	0.009	0.926
T_Baseline_Temporal_Inf_Post_L Normalized (ROI) AAL Atlas	46.56365	5.241818	47.38966	6.034286	1.76	1.626	0.203
T_Baseline_Temporal_Inf_Post_R Normalized (ROI) AAL Atlas	42.7455	5.122274	43.04091	6.2777	0.69	0.21	0.647
T_Baseline_Temporal_Mid_Ant_L Normalized (ROI) AAL Atlas	49.02475	5.428854	53.12528	7.10501	8.03	34.399	0.000
T_Baseline_Temporal_Mid_Ant_R Normalized (ROI) AAL Atlas	46.04345	4.885075	48.21686	6.839747	4.61	11.36	0.001
T_Baseline_Temporal_Mid_Mid_L Normalized (ROI) AAL Atlas	50.32828	5.456443	56.02565	8.233319	10.71	58.936	0.000
T_Baseline_Temporal_Mid_Mid_R Normalized (ROI) AAL Atlas	47.9686	5.127137	52.06921	7.951018	8.20	33.784	0.000
T_Baseline_Temporal_Mid_Post_L Normalized (ROI) AAL Atlas	50.53501	5.329212	56.33076	8.291416	10.85	62.292	0.000
T_Baseline_Temporal_Mid_Post_R Normalized (ROI) AAL Atlas	47.4043	5.125735	50.70885	7.457654	6.74	23.147	0.000
T_Baseline_Temporal_Pole_Mid_L Normalized (ROI) AAL Atlas	38.24755	5.566983	36.96262	6.195669	3.42	3.557	0.060
T_Baseline_Temporal_Pole_Mid_R Normalized (ROI) AAL Atlas	36.74488	5.170814	34.6405	6.179352	5.90	10.604	0.001
T_Baseline_Temporal_Pole_Sup_L Normalized (ROI) AAL Atlas	45.10772	4.912868	48.92297	6.586123	8.11	35.746	0.000
T_Baseline_Temporal_Pole_Sup_R Normalized (ROI) AAL Atlas	42.44217	4.239272	45.37709	6.121793	6.68	26.853	0.000
T_Baseline_Temporal_Sup_Ant_L Normalized (ROI) AAL Atlas	51.83505	6.05537	59.46422	9.149601	13.71	85.709	0.000
T_Baseline_Temporal_Sup_Ant_R Normalized (ROI) AAL Atlas	48.88878	5.082781	54.98425	8.769211	11.74	68.898	0.000
T_Baseline_Temporal_Sup_Mid_L Normalized (ROI) AAL Atlas	54.01341	6.272058	61.99548	9.45831	13.76	87.595	0.000
T_Baseline_Temporal_Sup_Mid_R Normalized (ROI) AAL Atlas	51.34185	5.57549	58.40573	9.059785	12.87	81.345	0.000
T_Baseline_Temporal_Sup_Post_L Normalized (ROI) AAL Atlas	52.22645	5.959719	59.27808	9.03064	12.65	75.413	0.000
T_Baseline_Temporal_Sup_Post_R Normalized (ROI) AAL Atlas	49.91907	5.588307	55.49242	8.647302	10.57	52.633	0.000
T_Baseline_Thalamus_L Normalized (ROI) AAL Atlas	56.54178	7.086691	66.49646	10.550377	16.18	107.86	0.000
T_Baseline_Thalamus_R Normalized (ROI) AAL Atlas	55.39783	6.90068	65.2625	10.420778	16.35	110.394	0.000
T_Baseline_Vermis_1_2 Normalized (ROI) AAL Atlas	50.44692	7.100393	57.97086	10.96509	13.88	51.192	0.000
T_Baseline_Vermis_10 Normalized (ROI) AAL Atlas	55.75287	8.896319	67.93821	13.265072	19.70	101.343	0.000
T_Baseline_Vermis_3 Normalized (ROI) AAL Atlas	52.25786	7.408513	60.30548	10.9761	14.30	64.758	0.000
T_Baseline_Vermis_4_5 Normalized (ROI) AAL Atlas	57.08649	7.413429	65.81621	11.237542	14.21	74.67	0.000
T_Baseline_Vermis_6 Normalized (ROI) AAL Atlas	59.55606	7.318832	65.98924	9.525346	10.25	46.768	0.000
T_Baseline_Vermis_7 Normalized (ROI) AAL Atlas	55.8715	7.881006	58.89977	9.647672	5.28	9.311	0.002
T_Baseline_Vermis_8 Normalized (ROI) AAL Atlas	54.87529	7.184679	57.43593	8.707734	4.56	8.061	0.005

(*Continued*)

Table 1
(*Continued*)

Brain region	Mean Perfusion in Marijuana	Standard Deviation in Marijuana	Mean Perfusion in Control	Standard Deviation in Control	% Difference	F-value	*p*-value
T_Baseline_Vermis_9 Normalized (ROI) AAL Atlas	61.31183	7.870997	68.99972	10.035826	11.80	58.567	0.000
T_Concentration_Amygdala_L Normalized (ROI) AAL Atlas	49.85022	5.923547	55.83307	7.354009	11.32	78.774	0.000
T_Concentration_Amygdala_R Normalized (ROI) AAL Atlas	49.47965	6.066876	55.86177	7.412376	12.12	86.493	0.000
T_Concentration_Angular_L Normalized (ROI) AAL Atlas	47.73449	4.91787	49.75447	5.467583	4.14	14.092	0.000
T_Concentration_Angular_R Normalized (ROI) AAL Atlas	43.9328	4.599118	44.52821	4.873009	1.35	1.444	0.230
T_Concentration_Calcarine_L Normalized (ROI) AAL Atlas	51.18401	5.064574	53.21756	6.005834	3.90	12.88	0.000
T_Concentration_Calcarine_R Normalized (ROI) AAL Atlas	52.09606	5.750411	56.72385	6.450033	8.51	53.781	0.000
T_Concentration_Caudate_L Normalized (ROI) AAL Atlas	49.07272	6.508982	54.19309	7.697805	9.92	49.535	0.000
T_Concentration_Caudate_R Normalized (ROI) AAL Atlas	50.60784	6.326911	56.90474	6.936625	11.71	83.499	0.000
T_Concentration_Cerebellum_10_L Normalized (ROI) AAL Atlas	38.36832	6.266902	41.42503	6.126199	7.66	21.36	0.000
T_Concentration_Cerebellum_10_R Normalized (ROI) AAL Atlas	35.60025	6.374343	38.05099	6.79234	6.65	12.689	0.000
T_Concentration_Cerebellum_3_L Normalized (ROI) AAL Atlas	51.47256	6.634569	55.83892	7.325716	8.14	36.343	0.000
T_Concentration_Cerebellum_3_R Normalized (ROI) AAL Atlas	50.30087	6.312668	54.2309	7.42586	7.52	31.143	0.000
T_Concentration_Cerebellum_4_5_L Normalized (ROI) AAL Atlas	54.04858	6.493161	59.25004	7.729147	9.18	51.126	0.000
T_Concentration_Cerebellum_4_5_R Normalized (ROI) AAL Atlas	54.91854	6.665596	59.68096	7.968101	8.31	40.546	0.000
T_Concentration_Cerebellum_6_L Normalized (ROI) AAL Atlas	60.04651	7.152467	66.7948	8.564999	10.64	70.615	0.000
T_Concentration_Cerebellum_6_R Normalized (ROI) AAL Atlas	58.92376	7.055112	65.12337	8.136715	10.00	62.916	0.000
T_Concentration_Cerebellum_7b_L Normalized (ROI) AAL Atlas	38.82732	6.038662	38.04399	6.264931	2.04	1.468	0.226
T_Concentration_Cerebellum_7b_R Normalized (ROI) AAL Atlas	31.259	5.888659	30.38275	5.90315	2.84	1.972	0.161
T_Concentration_Cerebellum_8_L Normalized (ROI) AAL Atlas	43.54307	6.213404	42.90355	6.564744	1.48	0.914	0.340
T_Concentration_Cerebellum_8_R Normalized (ROI) AAL Atlas	39.61891	5.763113	39.06905	6.441926	1.40	0.758	0.385
T_Concentration_Cerebellum_9_L Normalized (ROI) AAL Atlas	48.75722	6.770851	49.94111	7.163024	2.40	2.636	0.105
T_Concentration_Cerebellum_9_R Normalized (ROI) AAL Atlas	48.53009	6.183259	50.00876	7.24501	3.00	4.608	0.032
T_Concentration_Cerebellum_Crus1_L Normalized (ROI) AAL Atlas	50.91591	5.466004	51.25573	6.569578	0.67	0.306	0.581
T_Concentration_Cerebellum_Crus1_R Normalized (ROI) AAL Atlas	45.02667	4.945521	44.81574	6.03896	0.47	0.142	0.706
T_Concentration_Cerebellum_Crus2_L Normalized (ROI) AAL Atlas	38.6567	6.513492	36.95853	6.456303	4.49	6.091	0.014
T_Concentration_Cerebellum_Crus2_R Normalized (ROI) AAL Atlas	33.61696	5.484488	32.38603	5.456092	3.73	4.505	0.034
T_Concentration_Cingulum_Ant_L Normalized (ROI) AAL Atlas	54.61279	7.480441	61.61023	8.426164	12.04	72.455	0.000
T_Concentration_Cingulum_Ant_R Normalized (ROI) AAL Atlas	50.70728	6.716667	57.0121	7.945359	11.71	70.518	0.000
T_Concentration_Cingulum_Mid_L Normalized (ROI) AAL Atlas	55.95633	6.866907	62.13533	7.472068	10.46	68.587	0.000
T_Concentration_Cingulum_Mid_R Normalized (ROI) AAL Atlas	53.76494	6.582585	59.66768	7.638106	10.41	65.239	0.000
T_Concentration_Cingulum_Post_L Normalized (ROI) AAL Atlas	53.73966	7.132838	60.93425	8.683016	12.55	79.735	0.000
T_Concentration_Cingulum_Post_R Normalized (ROI) AAL Atlas	48.87368	6.863749	56.31338	8.589411	14.15	90.171	0.000
T_Concentration_Cuneus_L Normalized (ROI) AAL Atlas	49.31659	5.519945	51.32776	5.935356	4.00	11.331	0.001
T_Concentration_Cuneus_R Normalized (ROI) AAL Atlas	49.42461	5.503128	51.81028	5.897862	4.71	16.074	0.000
T_Concentration_Frontal_Inf_Oper_L Normalized (ROI) AAL Atlas	52.07736	6.090077	56.02483	6.441209	7.30	36.233	0.000
T_Concentration_Frontal_Inf_Oper_R Normalized (ROI) AAL Atlas	50.43051	5.370895	53.58128	5.849762	6.06	29.134	0.000
T_Concentration_Frontal_Inf_Orb_L Normalized (ROI) AAL Atlas	49.29301	5.200363	50.54536	5.266943	2.51	5.133	0.024
T_Concentration_Frontal_Inf_Orb_R Normalized (ROI) AAL Atlas	46.18596	4.829639	46.92857	5.069637	1.60	2.048	0.153
T_Concentration_Frontal_Inf_Tri_L Normalized (ROI) AAL Atlas	50.9744	5.52462	54.26101	5.721335	6.25	30.915	0.000
T_Concentration_Frontal_Inf_Tri_R Normalized (ROI) AAL Atlas	47.05297	4.625374	49.03514	5.011356	4.13	15.6	0.000
T_Concentration_Frontal_Mid_L Normalized (ROI) AAL Atlas	48.09328	5.119408	49.54621	5.098141	2.98	7.199	0.008

T_Concentration_Frontal_Mid_Orb_L Normalized (ROI) AAL Atlas	55.291	6.319451	58.07803	6.037572	4.92	17.786	0.000
T_Concentration_Frontal_Mid_Orb_L_9 Normalized (ROI) AAL Atlas	47.17735	5.537399	47.11361	6.194235	0.14	0.011	0.916
T_Concentration_Frontal_Mid_Orb_R Normalized (ROI) AAL Atlas	52.86368	6.16467	57.519	5.964747	8.43	51.791	0.000
T_Concentration_Frontal_Mid_Orb_R_10 Normalized (ROI) AAL Atlas	44.28936	5.959141	43.08147	6.635738	2.76	3.428	0.065
T_Concentration_Frontal_Mid_R Normalized (ROI) AAL Atlas	46.24978	4.838516	47.45694	5.155705	2.58	5.343	0.021
T_Concentration_Frontal_Sup_L Normalized (ROI) AAL Atlas	44.35378	4.883447	45.23578	4.640308	1.97	2.991	0.084
T_Concentration_Frontal_Sup_Medial_L Normalized (ROI) AAL Atlas	48.81763	5.543101	49.9262	5.407328	2.25	3.616	0.058
T_Concentration_Frontal_Sup_Medial_R Normalized (ROI) AAL Atlas	46.8719	5.217933	47.8633	5.123166	2.09	3.252	0.072
T_Concentration_Frontal_Sup_Orb_L Normalized (ROI) AAL Atlas	48.55344	5.465877	50.14023	5.818615	3.22	7.239	0.007
T_Concentration_Frontal_Sup_Orb_R Normalized (ROI) AAL Atlas	46.80076	5.325058	47.83688	5.987774	2.19	3.139	0.077
T_Concentration_Frontal_Sup_R Normalized (ROI) AAL Atlas	43.98066	4.752287	45.05208	4.926301	2.41	4.438	0.036
T_Concentration_Fusiform_L Normalized (ROI) AAL Atlas	51.13808	5.479952	54.77483	6.294312	6.87	35.987	0.000
T_Concentration_Fusiform_R Normalized (ROI) AAL Atlas	50.1023	5.599745	53.68723	6.19336	6.91	34.352	0.000
T_Concentration_Heschl_L Normalized (ROI) AAL Atlas	56.55361	7.099184	61.62213	7.714865	8.58	43.215	0.000
T_Concentration_Heschl_R Normalized (ROI) AAL Atlas	57.03432	7.359633	63.15284	7.797453	10.18	59.542	0.000
T_Concentration_Hippocampus_L Normalized (ROI) AAL Atlas	49.17531	5.823896	55.14161	7.140546	11.44	81.813	0.000
T_Concentration_Hippocampus_R Normalized (ROI) AAL Atlas	48.98878	6.032028	55.79564	7.379828	12.99	99.427	0.000
T_Concentration_Insula_L Normalized (ROI) AAL Atlas	55.7534	6.804083	61.43725	7.451596	9.70	58.867	0.000
T_Concentration_Insula_R Normalized (ROI) AAL Atlas	56.66812	7.00794	62.49023	7.309624	9.77	60.032	0.000
T_Concentration_Lingual_L Normalized (ROI) AAL Atlas	53.90882	5.761145	58.6477	6.574898	8.42	55.529	0.000
T_Concentration_Lingual_R Normalized (ROI) AAL Atlas	52.94538	5.737353	57.74837	6.64737	8.68	56.918	0.000
T_Concentration_Occipital_Inf_L Normalized (ROI) AAL Atlas	44.82963	5.08955	44.58648	6.480429	0.54	0.173	0.678
T_Concentration_Occipital_Inf_R Normalized (ROI) AAL Atlas	38.40973	5.282145	36.16122	6.018205	6.03	14.888	0.000
T_Concentration_Occipital_Mid_L Normalized (ROI) AAL Atlas	45.31114	4.608277	46.40419	5.605376	2.38	4.412	0.036
T_Concentration_Occipital_Mid_R Normalized (ROI) AAL Atlas	41.98987	4.890314	41.38021	5.31168	1.46	1.318	0.252
T_Concentration_Occipital_Sup_L Normalized (ROI) AAL Atlas	43.32759	4.760811	44.09506	5.494847	1.76	2.116	0.146
T_Concentration_Occipital_Sup_R Normalized (ROI) AAL Atlas	43.59775	4.881069	44.04904	5.275938	1.03	0.727	0.394
T_Concentration_Olfactory_L Normalized (ROI) AAL Atlas	51.9173	6.357895	56.94531	7.390782	9.24	50.677	0.000
T_Concentration_Olfactory_R Normalized (ROI) AAL Atlas	52.80441	6.340789	58.16235	6.982335	9.66	60.018	0.000
T_Concentration_Pallidum_L Normalized (ROI) AAL Atlas	55.72579	7.678517	63.96213	9.262705	13.76	90.782	0.000
T_Concentration_Pallidum_R Normalized (ROI) AAL Atlas	58.96949	8.495464	67.40758	9.477561	13.35	82.218	0.000
T_Concentration_Paracentral_Lobule_L Normalized (ROI) AAL Atlas	40.10006	4.889488	43.66687	6.109192	8.52	40.892	0.000
T_Concentration_Paracentral_Lobule_R Normalized (ROI) AAL Atlas	42.15938	4.983037	45.84571	6.200859	8.38	42.185	0.000
T_Concentration_ParaHippocampal_L Normalized (ROI) AAL Atlas	45.8693	5.004041	49.19638	5.566333	7.00	36.912	0.000
T_Concentration_ParaHippocampal_R Normalized (ROI) AAL Atlas	48.72419	5.442696	53.55666	6.420877	9.45	63.215	0.000
T_Concentration_Parietal_Inf_L Normalized (ROI) AAL Atlas	48.04493	5.284269	50.03026	5.715794	4.05	12.003	0.001
T_Concentration_Parietal_Inf_R Normalized (ROI) AAL Atlas	44.10484	5.371632	44.34829	5.680752	0.55	0.177	0.674
T_Concentration_Parietal_Sup_L Normalized (ROI) AAL Atlas	38.79084	4.56272	39.19294	4.965724	1.03	0.658	0.418
T_Concentration_Parietal_Sup_R Normalized (ROI) AAL Atlas	34.25501	4.232943	33.55245	4.761659	2.07	2.283	0.132
T_Concentration_Postcentral_L Normalized (ROI) AAL Atlas	45.21702	4.785556	48.10216	5.375858	6.18	30.152	0.000
T_Concentration_Postcentral_R Normalized (ROI) AAL Atlas	42.02254	4.378001	43.63371	5.09147	3.76	10.971	0.001
T_Concentration_Precentral_L Normalized (ROI) AAL Atlas	46.3021	4.796004	49.37936	5.556135	6.43	33.439	0.000
T_Concentration_Precentral_R Normalized (ROI) AAL Atlas	43.65604	4.408549	45.79641	5.04226	4.79	19.316	0.000
T_Concentration_Precuneus_L Normalized (ROI) AAL Atlas	47.60587	5.201194	51.6757	6.211321	8.20	48.667	0.000
T_Concentration_Precuneus_R Normalized (ROI) AAL Atlas	49.1711	5.618049	54.00761	6.550148	9.38	59.928	0.000

(*Continued*)

Table 1
(*Continued*)

Brain region	Mean Perfusion in Marijuana	Standard Deviation in Marijuana	Mean Perfusion in Control	Standard Deviation in Control	% Difference	F-value	*p*-value
T_Concentration_Putamen_L Normalized (ROI) AAL Atlas	59.69849	7.550099	67.06395	8.757219	11.62	77.235	0.000
T_Concentration_Putamen_R Normalized (ROI) AAL Atlas	60.2217	7.79234	67.63776	8.399456	11.60	77.189	0.000
T_Concentration_Rectus_L Normalized (ROI) AAL Atlas	52.82645	6.263625	55.40957	6.598362	4.77	14.703	0.000
T_Concentration_Rectus_R Normalized (ROI) AAL Atlas	51.88476	6.071728	55.28853	6.559261	6.35	26.744	0.000
T_Concentration_Rolandic_Oper_L Normalized (ROI) AAL Atlas	54.19989	6.591981	59.65611	7.415117	9.58	56.781	0.000
T_Concentration_Rolandic_Oper_R Normalized (ROI) AAL Atlas	52.38221	5.91648	57.48823	6.836017	9.29	60.607	0.000
T_Concentration_Supp_Motor_Area_L Normalized (ROI) AAL Atlas	45.70649	5.233241	49.05838	6.599732	7.07	31.298	0.000
T_Concentration_Supp_Motor_Area_R Normalized (ROI) AAL Atlas	45.62076	5.289635	49.39773	6.411959	7.95	40.084	0.000
T_Concentration_SupraMarginal_L Normalized (ROI) AAL Atlas	50.80645	5.587681	54.41037	6.516462	6.85	33.631	0.000
T_Concentration_SupraMarginal_R Normalized (ROI) AAL Atlas	47.70499	5.14395	49.73397	6.043164	4.16	12.513	0.000
T_Concentration_Temporal_Inf_Ant_L Normalized (ROI) AAL Atlas	41.30516	6.179724	39.16987	7.28042	5.31	9.583	0.002
T_Concentration_Temporal_Inf_Ant_R Normalized (ROI) AAL Atlas	36.61733	5.692009	34.94786	6.017634	4.67	7.421	0.007
T_Concentration_Temporal_Inf_Mid_L Normalized (ROI) AAL Atlas	44.7564	5.24256	44.12887	6.005597	1.41	1.173	0.279
T_Concentration_Temporal_Inf_Mid_R Normalized (ROI) AAL Atlas	40.97618	4.871399	40.63647	5.522756	0.83	0.401	0.527
T_Concentration_Temporal_Inf_Post_L Normalized (ROI) AAL Atlas	46.78993	4.866223	46.63438	5.602805	0.33	0.083	0.773
T_Concentration_Temporal_Inf_Post_R Normalized (ROI) AAL Atlas	42.68486	4.80827	42.2856	5.496783	0.94	0.565	0.453
T_Concentration_Temporal_Mid_Ant_L Normalized (ROI) AAL Atlas	49.80547	5.296784	53.20411	6.234757	6.60	33.067	0.000
T_Concentration_Temporal_Mid_Ant_R Normalized (ROI) AAL Atlas	46.52308	4.735196	48.54641	5.910537	4.26	14.041	0.000
T_Concentration_Temporal_Mid_Mid_L Normalized (ROI) AAL Atlas	50.87185	5.386462	54.56373	6.512517	7.00	37.004	0.000
T_Concentration_Temporal_Mid_Mid_R Normalized (ROI) AAL Atlas	48.50412	4.981549	51.55393	5.927962	6.10	29.869	0.000
T_Concentration_Temporal_Mid_Post_L Normalized (ROI) AAL Atlas	50.62314	5.233584	54.27736	6.182103	6.97	39.057	0.000
T_Concentration_Temporal_Mid_Post_R Normalized (ROI) AAL Atlas	47.4793	5.08385	49.20977	5.511857	3.58	9.838	0.002
T_Concentration_Temporal_Pole_Mid_L Normalized (ROI) AAL Atlas	38.83897	5.29551	37.4947	6.041719	3.52	5.29	0.022
T_Concentration_Temporal_Pole_Mid_R Normalized (ROI) AAL Atlas	37.21195	5.003259	36.16489	5.787386	2.85	3.561	0.060
T_Concentration_Temporal_Pole_Sup_L Normalized (ROI) AAL Atlas	45.78811	4.748887	48.54483	5.620347	5.84	26.96	0.000
T_Concentration_Temporal_Pole_Sup_R Normalized (ROI) AAL Atlas	42.74936	4.324909	45.51549	5.085355	6.27	32.879	0.000
T_Concentration_Temporal_Sup_Ant_L Normalized (ROI) AAL Atlas	52.61724	6.202435	57.88399	7.485392	9.53	56.873	0.000
T_Concentration_Temporal_Sup_Ant_R Normalized (ROI) AAL Atlas	49.14629	5.181445	54.02296	6.680107	9.45	66.417	0.000
T_Concentration_Temporal_Sup_Mid_L Normalized (ROI) AAL Atlas	54.41598	6.355222	59.9346	7.422592	9.65	60.898	0.000
T_Concentration_Temporal_Sup_Mid_R Normalized (ROI) AAL Atlas	51.69801	5.536063	56.82909	6.9193	9.46	65.995	0.000
T_Concentration_Temporal_Sup_Post_L Normalized (ROI) AAL Atlas	52.74995	5.993976	57.75666	7.092064	9.06	55.83	0.000
T_Concentration_Temporal_Sup_Post_R Normalized (ROI) AAL Atlas	50.40924	5.441043	54.20897	6.260213	7.26	39.802	0.000
T_Concentration_Thalamus_L Normalized (ROI) AAL Atlas	57.04013	7.280588	63.8685	8.245438	11.30	72.571	0.000
T_Concentration_Thalamus_R Normalized (ROI) AAL Atlas	55.67416	7.094491	62.73679	7.893742	11.93	82.737	0.000
T_Concentration_Vermis_1_2 Normalized (ROI) AAL Atlas	51.45749	7.17461	56.12413	7.288862	8.68	32.507	0.000
T_Concentration_Vermis_10 Normalized (ROI) AAL Atlas	56.03549	8.919071	65.55753	10.498396	15.66	90.967	0.000
T_Concentration_Vermis_3 Normalized (ROI) AAL Atlas	52.56592	7.500432	58.61169	8.465327	10.88	53.728	0.000
T_Concentration_Vermis_4_5 Normalized (ROI) AAL Atlas	57.48862	7.580116	63.95649	8.935264	10.65	58.415	0.000
T_Concentration_Vermis_6 Normalized (ROI) AAL Atlas	59.68063	7.170711	64.93489	7.467759	8.43	46.743	0.000
T_Concentration_Vermis_7 Normalized (ROI) AAL Atlas	55.99778	7.79746	58.13288	8.323427	3.74	6.429	0.012
T_Concentration_Vermis_8 Normalized (ROI) AAL Atlas	55.36944	7.548706	57.6116	9.10618	3.97	6.961	0.009
T_Concentration_Vermis_9 Normalized (ROI) AAL Atlas	61.84872	7.769693	67.75096	8.740072	9.11	47.826	0.000

Table 2
Top 10 predictive regions from brain SPECT distinguishing marijuana users from healthy controls

mRMR Features
R Hippocampus on Concentration SPECT
Left anterior inferior temporal cortex Baseline SPECT
Right inferior occipital cortex Concentration SPECT
Right Paracentral Lobule Baseline SPECT
Left Cerebellum Subregion 10 Concentration SPECT
Left Cerebellum Subregion 7B Concentration SPECT
Left Anterior mid temporal cortex Concentration SPECT
Left Pallidum Subregion 10 Baseline SPECT
Right Cerebellum Subregion 10 Concentration SPECT
Right Posterior Cingulate Gyrus Concentration SPECT

frontal lobes, inferior parietal cortex, and fusiform gyrus at baseline [38]. This same study also showed impaired response to methyphenidate stimulant challenge in female cannabis users in the cerebellum, medial frontal gyrus, pons, hippocampus, thalamus, and midbrain. A perfusion MRI study with arterial spin labeling also showed temporal lobe hypoperfusion in 23 adolescent marijuana users compared to 23 age-matched controls [39]. These perfusion differences persisted after four weeks of abstinence suggesting that the effects of marijuana on brain hypoperfusion may be long term.

A trimmed means approach was used to estimate cerebral perfusion from the brain SPECT scans of our study participants. The main advantage of this method is in its robustness, lowering partial volume effects while protecting against outliers [40, 41]. In excluding such information, the resulting dataset may not as closely resemble the original data but this issue is less likely in larger datasets such as in our sample.

There are several implications for this work. First, marijuana users have lower cerebral perfusion than non-users. Second, the most predictive region separating these two groups is hippocampal hypoperfusion on concentration SPECT imaging. This work suggests that marijuana use has potentially deleterious influences in the brain—particularly regions important in memory and learning and known to be affected by AD. The main advantage of our study is the large sample size, application of different algorithms to confirm consistency of results, and subgroup analysis to account for co-morbidities. The main disadvantage of our study is its cross sectional design. An additional caveat to consider is that brain atrophy from marijuana use could be driving the hippocampal hypoperfusion results given its vulnerability to atrophy [42]. Future work combining structural and functional imaging may better elucidate this relationship.

However, such results may give pause to the continued promotion of a substance that may be harmful to users, especially if used for the intention of therapeutic purposes. Longitudinal studies are required at the pre-teen, high school, and college level to better characterize the time course of such alterations. Based upon the results of our study, doubts remain as to the application of marijuana in treatment of AD, as some have suggested [4].

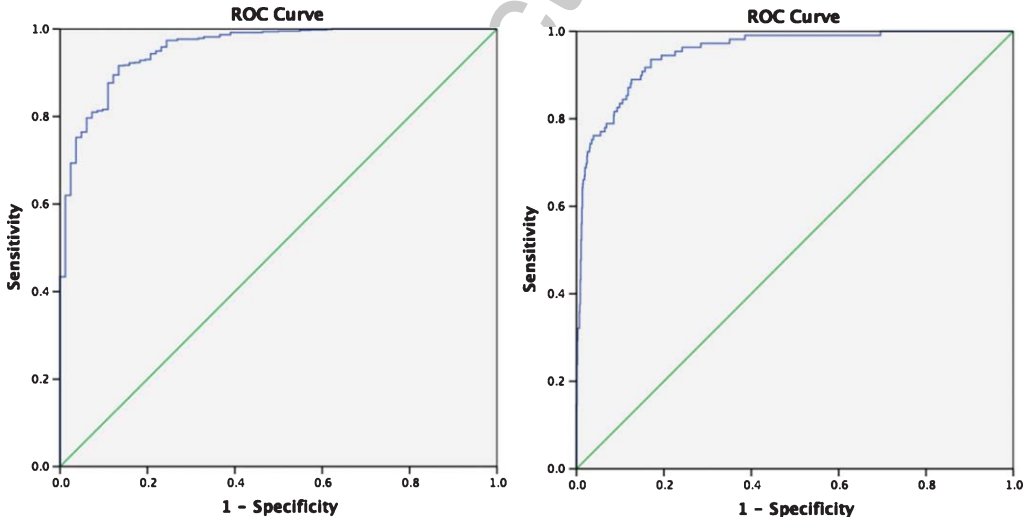

Fig. 1. Receiver operating characteristic (ROC) results of perfusion regions of interest in separating marijuana users from controls. (A) ROC Curve of Baseline Perfusion ROIs in Separating Marijuana Users From Controls. (B) ROC Curve of Concentration Perfusion ROIs in Separating Marijuana Users From Controls.

DISCLOSURE STATEMENT

Authors' disclosures available online (http://j-alz.com/manuscript-disclosures/160833).

REFERENCES

[1] Hasin DS, Saha TD, Kerridge BT, Goldstein RB, Chou SP, Zhang H, Jung J, Pickering RP, Ruan WJ, Smith SM, Huang B, Grant BF (2015) Prevalence of marijuana use disorders in the United States Between 2001-2002 and 2012-2013. *JAMA Psychiatry* **72**, 1235-1242.

[2] Maas A (2016) Traumatic brain injury: Changing concepts and approaches. *Chin J Traumatol* **19**, 3-6.

[3] Grotenhermen F, Muller-Vahl K (2012) The therapeutic potential of cannabis and cannabinoids. *Dtsch Arztebl Int* **109**, 495-501.

[4] Maust DT, Bonar EE, Ilgen MA, Blow FC, Kales HC (2016) Agitation in Alzheimer disease as a qualifying condition for medical marijuana in the United States. *Am J Geriatr Psychiatry* **24**, 1000-1003.

[5] American Academy of Neurology, Position Statement: Use of Medical Marijuana for Neurologic Disorders., https://www.aan.com/uploadedFiles/Website_Library_Assets/Documents/6.Public_Policy/1.Stay_Informed/2.Position_Statements/3.PDFs_of_all_Position_Statements/Final Medical Marijuana Position Statement.pdf, Accessed 7/31-2016.

[6] Antonsdottir IM, Makino KM, Porsteinsson AP (2016) Dazed and confused: Medical cannabis in Alzheimer disease. *Am J Geriatr Psychiatry* **24**, 1004-1006.

[7] Volkow ND, Compton WM, Weiss SR (2014) Adverse health effects of marijuana use. *N Engl J Med* **371**, 879.

[8] Volkow ND, Swanson JM, Evins AE, DeLisi LE, Meier MH, Gonzalez R, Bloomfield MA, Curran HV, Baler R (2016) Effects of cannabis use on human behavior, including cognition, motivation, and psychosis: A review. *JAMA Psychiatry* **73**, 292-297.

[9] van de Giessen E, Weinstein JJ, Cassidy CM, Haney M, Dong Z, Ghazzaoui R, Ojeil N, Kegeles LS, Xu X, Vadhan NP, Volkow ND, Slifstein M, Abi-Dargham A (2016) Deficits in striatal dopamine release in cannabis dependence. *Mol Psychiatry*. doi: 10.1038/mp.2016.21

[10] Rigucci S, Marques TR, Di Forti M, Taylor H, Dell'Acqua F, Mondelli V, Bonaccorso S, Simmons A, David AS, Girardi P, Pariante CM, Murray RM, Dazzan P (2016) Effect of high-potency cannabis on corpus callosum microstructure. *Psychol Med* **46**, 841-854.

[11] Filbey FM, Aslan S, Calhoun VD, Spence JS, Damaraju E, Caprihan A, Segall J (2014) Long-term effects of marijuana use on the brain. *Proc Natl Acad Sci U S A* **111**, 16913-16918.

[12] Currais A, Quehenberger O, Armando AM, Daugherty D, Maher P, Schubert D (2016) Amyloid proteotoxicity initiates an inflammatory response blocked by cannabinoids. *NPJ Aging Mech Dis* **2**, 16012.

[13] Ashtari M, Avants B, Cyckowski L, Cervellione KL, Roofeh D, Cook P, Gee J, Sevy S, Kumra S (2011) Medial temporal structures and memory functions in adolescents with heavy cannabis use. *J Psychiatr Res* **45**, 1055-1066.

[14] Cousijn J, Wiers RW, Ridderinkhof KR, van den Brink W, Veltman DJ, Goudriaan AE (2012) Grey matter alterations associated with cannabis use: Results of a VBM study in heavy cannabis users and healthy controls. *Neuroimage* **59**, 3845-3851.

[15] Yucel M, Solowij N, Respondek C, Whittle S, Fornito A, Pantelis C, Lubman DI (2008) Regional brain abnormalities associated with long-term heavy cannabis use. *Arch Gen Psychiatry* **65**, 694-701.

[16] Amen DG, Raji CA, Willeumier K, Taylor D, Tarzwell R, Newberg A, Henderson TA (2015) Functional neuroimaging distinguishes posttraumatic stress disorder from traumatic brain injury in focused and large community datasets. *PLoS One* **10**, e0129659.

[17] Raji CA, Willeumier K, Taylor D, Tarzwell R, Newberg A, Henderson TA, Amen DG (2015) Functional neuroimaging with default mode network regions distinguishes PTSD from TBI in a military veteran population. *Brain Imaging Behav* **9**, 527-534.

[18] Mazziotta J, Toga A, Evans A, Fox P, Lancaster J, Zilles K, Woods R, Paus T, Simpson G, Pike B, Holmes C, Collins L, Thompson P, MacDonald D, Iacoboni M, Schormann T, Amunts K, Palomero-Gallagher N, Geyer S, Parsons L, Narr K, Kabani N, Le Goualher G, Boomsma D, Cannon T, Kawashima R, Mazoyer B (2001) A probabilistic atlas and reference system for the human brain: International Consortium for Brain Mapping (ICBM). *Philos Trans R Soc Lond B Biol Sci* **356**, 1293-1322.

[19] Chang W, Henkin RE, Buddemeyer E (1984) The sources of overestimation in the quantification by SPECT of uptakes in a myocardial phantom: Concise communication. *J Nucl Med* **25**, 788-791.

[20] Tzourio-Mazoyer N, Landeau B, Papathanassiou D, Crivello F, Etard O, Delcroix N, Mazoyer B, Joliot M (2002) Automated anatomical labeling of activations in SPM using a macroscopic anatomical parcellation of the MNI MRI single-subject brain. *Neuroimage* **15**, 273-289.

[21] Amen DG, Willeumier K, Omalu B, Newberg A, Raghavendra C, Raji CA (2016) Perfusion neuroimaging abnormalities alone distinguish National Football League players from a healthy population. *J Alzheimers Dis* **53**, 237-241.

[22] Benjamini Y, Hochberg Y (1995) Controlling the false discovery rate: A practical and powerful approach to multiple testing. *J R Stat Soc Series B Stat Methodol* **57**, 289-300.

[23] Cohen J (1988) Statistical Power Analysis for the Behavioral Sciences, 2nd Ed., Lawrence Erlbaum Associates, Hillsdale, NJ.

[24] Moller C, Pijnenburg YA, van der Flier WM, Versteeg A, Tijms B, de Munck JC, Hafkemeijer A, Rombouts SA, van der Grond J, van Swieten J, Dopper E, Scheltens P, Barkhof F, Vrenken H, Wink AM (2015) Alzheimer disease and behavioral variant frontotemporal dementia: Automatic classification based on cortical atrophy for single-subject diagnosis. *Radiology* **279**, 838-848.

[25] Iniesta R, Stahl D, McGuffin P (2016) Machine learning, statistical learning and the future of biological research in psychiatry. *Psychol Med* **46**, 2455-2465.

[26] Ding C, Peng H (2005) Minimum redundancy feature selection from microarray gene expression data. *J Bioinform Comput Biol* **3**, 185-205.

[27] Yucel M, Lorenzetti V, Suo C, Zalesky A, Fornito A, Takagi MJ, Lubman DI, Solowij N (2016) Hippocampal harms, protection and recovery following regular cannabis use. *Transl Psychiatry* **6**, e710.

[28] Carey SE, Nestor L, Jones J, Garavan H, Hester R (2015) Impaired learning from errors in cannabis users: Dorsal

anterior cingulate cortex and hippocampus hypoactivity. *Drug Alcohol Depend* **155**, 175-182.

[29] Filbey FM, McQueeny T, Kadamangudi S, Bice C, Ketcherside A (2015) Combined effects of marijuana and nicotine on memory performance and hippocampal volume. *Behav Brain Res* **293**, 46-53.

[30] Navakkode S, Korte M (2014) Pharmacological activation of CB1 receptor modulates long term potentiation by interfering with protein synthesis. *Neuropharmacology* **79**, 525-533.

[31] Ganzer F, Broning S, Kraft S, Sack PM, Thomasius R (2016) Weighing the evidence: A systematic review on long-term neurocognitive effects of cannabis use in abstinent adolescents and adults. *Neuropsychol Rev* **26**, 186-222.

[32] Schrot RJ, Hubbard JR (2016) Cannabinoids: Medical implications. *Ann Med* **48**, 128-141.

[33] Orr JM, Paschall CJ, Banich MT (2016) Recreational marijuana use impacts white matter integrity and subcortical (but not cortical) morphometry. *Neuroimage Clin* **12**, 47-56.

[34] Blanco-Hinojo L, Pujol J, Harrison BJ, Macia D, Batalla A, Nogue S, Torrens M, Farre M, Deus J, Martin-Santos R (2016) Attenuated frontal and sensory inputs to the basal ganglia in cannabis users. *Addict Biol*. doi: 10.1111/adb.12370

[35] Heitzeg MM, Cope LM, Martz ME, Hardee JE, Zucker RA (2015) Brain activation to negative stimuli mediates a relationship between adolescent marijuana use and later emotional functioning. *Dev Cogn Neurosci* **16**, 71-83.

[36] O'Leary DS, Block RI, Koeppel JA, Flaum M, Schultz SK, Andreasen NC, Ponto LB, Watkins GL, Hurtig RR, Hichwa RD (2002) Effects of smoking marijuana on brain perfusion and cognition. *Neuropsychopharmacology* **26**, 802-816.

[37] Vaidya JG, Block RI, O'Leary DS, Ponto LB, Ghoneim MM, Bechara A (2012) Effects of chronic marijuana use on brain activity during monetary decision-making. *Neuropsychopharmacology* **37**, 618-629.

[38] Wiers CE, Shokri-Kojori E, Wong CT, Abi-Dargham A, Demiral SB, Tomasi D, Wang GJ, Volkow ND (2016) Cannabis abusers show hypofrontality and blunted brain responses to a stimulant challenge in females but not in males. *Neuropsychopharmacology* **41**, 2596-2605.

[39] Jacobus J, Goldenberg D, Wierenga CE, Tolentino NJ, Liu TT, Tapert SF (2012) Altered cerebral blood flow and neurocognitive correlates in adolescent cannabis users. *Psychopharmacology (Berl)* **222**, 675-684.

[40] Li X (2013) Functional Magnetic Resonance Imaging Processing, Springer, Berlin.

[41] Tohka J, Zijdenbos A, Evans A (2004) Fast and robust parameter estimation for statistical partial volume models in brain MRI. *Neuroimage* **23**, 84-97.

[42] Lorenzetti V, Solowij N, Whittle S, Fornito A, Lubman DI, Pantelis C, Yucel M (2015) Gross morphological brain changes with chronic, heavy cannabis use. *Br J Psychiatry* **206**, 77-78.